Title

Soft gluon resummation in Higgs boson plus two jet production at the LHC

Authors

Sun, Peng

Yuan, C-P

Yuan, Feng

Publication Date

2019-10-01

DOI

10.1016/j.physletb.2019.134852

Peer reviewed

Physics Letters B 797 (2019) 134852

Contents lists available at ScienceDirect

Physics Letters B

www.elsevier.com/locate/physletb

Soft gluon resummation in Higgs boson plus two jet production at the LHC

Peng Sun [a,b,*], C.-P. Yuan [b], Feng Yuan [c]

[a] Department of Physics and Institute of Theoretical Physics, Nanjing Normal University, Nanjing, Jiangsu, 210023, China
[b] Department of Physics and Astronomy, Michigan State University, East Lansing, MI 48824, USA
[c] Nuclear Science Division, Lawrence Berkeley National Laboratory, Berkeley, CA 94720, USA

ARTICLE INFO

Article history:
Received 6 March 2019
Received in revised form 4 August 2019
Accepted 7 August 2019
Available online 12 August 2019
Editor: G.F. Giudice

ABSTRACT

The soft gluon resummation effect in the Higgs boson plus two-jet production at the LHC is studied by applying the transverse momentum dependent factorization formalism. The large logarithms, introduced by the small total transverse momentum of the Higgs boson plus two-jet final state system, are resummed to all orders in the expansion of the strong interaction coupling with the accuracy of Next-to-Leading Logarithm order. This significantly improves the theoretical prediction. We also compare our result with the prediction of the Monte Carlo event generator Pythia8, and find noticeable difference in the distributions of the total transverse momentum and the azimuthal angle correlations of the final state Higgs boson and two-jet system, when applying similar kinematic cuts used in the LHC data analysis. This difference is large enough to affect the measurement of Higgs boson coupling to the vector boson at the future High luminosity LHC.

1. Introduction

After the discovery of Higgs boson at the CERN Large Hadron Colllider (LHC) [1,2], determining its properties has become one of the most important tasks for the high energy physics community. It requires a careful comparison between the experimental measurements of various Higgs boson production and decay channels and the Standard Model (SM) predictions. Among these channels, the Higgs boson plus two jet production at the LHC is one of the most important ones to test the couplings of the Higgs boson [3–12], which can be expressed as:

$$A(P) + B(\bar{P}) \to H(P_H) + Jet(P_{J1}) + Jet(P_{J2}) + X\,, \qquad (1)$$

where P and $\bar{P}$ represent the incoming hadrons' momenta, P_H is the momentum of the final state Higgs boson, and the momenta of the final state jets are P_{J1} and P_{J2} with their rapidities y_{J1} and y_{J2}, respectively. In this production, the Higgs boson can be produced via two gluon fusion (GF) or two vector boson fusion (VBF) mechanisms. Being able to separate the GF and VBF production channels would help determining the couplings of Higgs boson, for they are sensitive to the effective coupling of Higgs boson to gluons and to weak gauge bosons, respectively. To achieve this gaol, we study the kinematic distributions of the Higgs boson and the two final state jets and their correlations. For example, the rapidity gap of the two final state jets ($|\Delta y_{JJ}| = |y_{J1} - y_{J2}|$) in the GF process tends to be smaller than that in the VBF process. Therefore, requiring a larger value of $|\Delta y_{JJ}|$ would enhance the relative contribution from VBF process [13].

In addition, the differential cross sections of the total transverse momentum ($\vec{q}_\perp = \vec{P}_H^\perp + \vec{P}_{J1}^\perp + \vec{P}_{J2}^\perp$) for the Higgs and the two final state jets are also sensitive to the production mechanisms. Such $q_\perp$ distributions are strongly dependent on the soft gluon radiations, especially in the small $q_\perp$ region. Since the effect of soft gluon radiations is determined by the color structures of the scattering processes, and the Higgs boson GF and VBF production mechanisms in this channel have different color structures, their $q_\perp$ distributions will peak at the different values. Hence, a precise theoretical prediction on the $q_\perp$ distribution is needed to separate the GF and VBF production processes. To reliably predict the $q_\perp$ distribution, soft gluon shower effect must be considered. The soft gluon shower effect brings the large Sudakov logarithms into all orders of the perturbative expansion, and then breaks the validity of the perturbative expansion. Fortunately, this problem can be resolved by performing an all-order transverse momentum

* Corresponding author.
E-mail addresses: pengsun@msu.edu (P. Sun), yuan@pa.msu.edu (C.-P. Yuan), fyuan@lbl.gov (F. Yuan).

https://doi.org/10.1016/j.physletb.2019.134852

dependent (TMD) resummation calculation based on the TMD factorization theorem [14–16], which is widely used to resum these large logarithms in color singlet processes [17]. For the processes with more complicated color structures, the TMD resummation was discussed firstly in Ref. [18] for colored heavy particle production processes. For the processes with massless jets in the final states, the extra soft gluon radiation could be within or outside the jet cone. Within the jet cone, the radiated gluon can be treated as a part of the jet, and it leads to a contribution for the bin of $q_\perp = 0$. If it is outside the jet cone, it will generate the large Sudakov logarithm, and it should be resummed. Its details can be found in the recently developed TMD resummation method [19–21].

In this work, we will apply the TMD resummation method to study the soft gluon resummation effect on the production of Higgs boson plus two jets in hadron collision. In terms of the TMD factorization formalism, the $q_\perp$ differential cross section is factorized into several individual factors which will be analytically calculated up to the one-loop order. As of today, the Monte Carlo (MC) event generators are the only available tools to predict the soft gluon shower effect for this channel. Our calculation not only, for the first time, provides an important test on the validity of the commonly used MC event generators, but also brings the accuracy of the theoretical prediction into the Next-to-Leading Logarithm (NLL) level.

2. TMD factorization

In our calculation, the effective Lagrangian in the heavy top quark mass limit is used to describe the effective coupling between Higgs boson and gluons [22],

$$\mathcal{L}_{eff} = -\frac{\alpha_s}{12\pi v} F^a_{\mu\nu} F^{a\mu\nu} H, \tag{2}$$

where v is the vacuum expectation value, H the Higgs boson field, $F^{\mu\nu}$ the gluon field strength tensor, and a the color index. Our TMD resummation formula can be written as:

$$\frac{d^6\sigma}{dy_H dy_{J1} dy_{J2} dP^2_{J1\perp} dP^2_{J2\perp} d^2\vec{q}_\perp} = \sum_{ab}\left[\int \frac{d^2\vec{b}}{(2\pi)^2} e^{-i\vec{q}_\perp\cdot\vec{b}} W_{ab\to Hcd}(x_1,x_2,b) + Y_{ab\to Hcd}\right], \tag{3}$$

where y_H, y_{J1} and y_{J2} denote the rapidities of the Higgs boson and the jets, respectively, $P_{J1\perp}$ and $P_{J2\perp}$ are the jets transverse momentum, and $\vec{q}_\perp = \vec{P}_{H\perp} + \vec{P}_{J1\perp} + \vec{P}_{J2\perp}$ is the imbalance transverse momentum of the Higgs boson and the two final state jets. The first term (W) contains all order resummation effect and the second term (Y) accounts for the difference between the fixed order result and the so-called asymptotic result which is given by expanding the resummation result to the same order in α_s as the fixed order term. x_1 and x_2 are the momentum fractions of the incoming hadrons carried by the incoming partons, with

$$x_{1,2} = \frac{\sqrt{m_H^2 + P^2_{H\perp}}e^{\pm y_H} + \sqrt{P^2_{J1\perp}}e^{\pm y_{J1}} + \sqrt{P^2_{J2\perp}}e^{\pm y_{J2}}}{\sqrt{S}}. \tag{4}$$

We can write the all order resummation result for W as

$$\begin{aligned} W_{ab\to Hcd}(x_1,x_2,b) &= x_1 f_a(x_1,\mu_F = b_0/b_*) x_2 f_b(x_2,\mu_F = b_0/b_*) \\ &\times e^{-S_{\rm Sud}(Q^2,\hat{\mu})} e^{-\mathcal{F}_{NP}(Q^2,b)} \\ &\times {\rm Tr}\left[\mathbf{H}_{ab\to Hcd}(\hat{\mu}) \exp\left[-\int_{b_0/b_*}^{\hat{\mu}} \frac{d\mu}{\mu}\gamma^{s\dagger}\right] \mathbf{S}_{ab\to Hcd}(b_0/b_*) \right. \\ &\left. \times \exp\left[-\int_{b_0/b_*}^{\hat{\mu}} \frac{d\mu}{\mu}\gamma^{s}\right]\right], \end{aligned} \tag{5}$$

where $s = x_1x_2S$, and S is the hadronic center of mass energy squared, $b_0 = 2e^{-\gamma_E}$, with γ_E being the Euler constant, $\hat{\mu}$ is the resummation scale to apply the TMD factorization in the resummation calculation, as in the Collins 2011 scheme [16]. We would like to emphasize that the above formula applies for both of VBF and GF channels. $f_{a,b}(x,\mu_F)$ are the parton distribution functions (PDFs) for the incoming partons a and b, and the μ_F is the evolution scale of the PDFs. The renormalization scale has been set as the mass of Higgs boson. $\mathbf{H}_{ab\to Hcd}$ is the hard factor, and it is a matrix based on a set of basis color factors. By applying the Catani-De Florian-Grazzini (CFG) scheme [23] and the TMD factorization in the Collins 2011 scheme [16], we obtain the color singlet component in the hard factor matrix $H^{VBF}_{ab\to Hcd}$ for the VBF channels, at the next-to-leading order (NLO), as

$$\begin{aligned} H^{(1)VBF}_{ab\to Hcd} = H^{(0)VBF}_{ab\to Hcd}\frac{C_F\alpha_s}{2\pi}\left[-\ln^2\left(\frac{\hat{\mu}^2}{\hat{t}_1}\right) - \ln^2\left(\frac{\hat{\mu}^2}{\hat{t}_2}\right)\right. \\ - 3\ln\left(\frac{\hat{\mu}^2}{\hat{t}_1}\right) - 3\ln\left(\frac{\mu^2}{\hat{t}_2}\right) - 16 \\ + \frac{1}{2}\ln^2\left(\frac{\hat{\mu}^2}{P^2_{J1\perp}}\right) + \frac{3}{2}\ln\left(\frac{\hat{\mu}^2}{R^2P^2_{J1\perp}}\right) \\ - \ln\left(R^2\right)\ln\left(\frac{\hat{\mu}^2}{P^2_{J1\perp}}\right) + \frac{13}{2} - \frac{2}{3}\pi^2 \\ + \frac{1}{2}\ln^2\left(\frac{\hat{\mu}^2}{P^2_{J2\perp}}\right) + \frac{3}{2}\ln\left(\frac{\hat{\mu}^2}{R^2P^2_{J2\perp}}\right) \\ \left. - \ln\left(R^2\right)\ln\left(\frac{\hat{\mu}^2}{P^2_{J2\perp}}\right) + \frac{13}{2} - \frac{2}{3}\pi^2\right], \end{aligned} \tag{6}$$

where R and $P_{J\perp i}$ denote the jet size and transverse momenta of the final state jets, and $H^{(0)}$ is the tree level cross section. Denoting the initial parton momenta as (p_a, p_b) and the final state jet momenta as (p_{j1}, p_{j2}), the above kinematic variables $\hat{t}_1$ and $\hat{t}_2$ can be expressed as $\hat{t}_1 = (p_a - p_{j1})^2$ and $\hat{t}_2 = (p_b - p_{j2})^2$. Similarly, we have $\hat{u}_1 = (p_a - p_{j2})^2$ and $\hat{u}_1 = (p_b - p_{j1})^2$. In the above hard factor, besides the contribution from the virtual correction at the one-loop order, we have also included two pieces of contributions from real gluon radiation. The first one is from the jet function, which describes the gluon radiation within the jet [24]. Here, we follow Ref. [24] and apply the dimensional regularization method to integrate the allowed phase space volume of the radiated gluon, and the anti-k_T jet algorithm is adopted. Another one comes from the ϵ-expansion terms in the soft gluon radiation out of the jet, which contributes to a finite term when Fourier transformed into b-space with the dimension $D = 4 - 2\epsilon$ [19]. Here, we make the light jet off-shell to regulate the collinear divergence associated with the soft gluon radiation at small transverse momentum $q_\perp$, which effectively excludes gluon radiation within the jet cone in the narrow jet approximation. As found in Ref. [20], the different treatment of the jet part in the jet functions and the soft factor leads to a finite contribution in the hard factor, which does not depend on the jet cone size. Numerically, it is found to

be approximately $\frac{\alpha_s}{2\pi}C_A(\frac{\pi^2}{6})$ and $\frac{\alpha_s}{2\pi}C_F(\frac{\pi^2}{6})$ for gluon and quark jet, respectively. We have included these additional contributions in the above equation, which were not included in Ref. [21]. For the VBF channel, in addition to the color singlet contribution, there is also a non-zero color-octet component in the hard factor matrix, at the α_s order. However, in the perturbative expansion it does not contribute until next-to-next-leading-order (NNLO). Hence, we ignore its contribution in this work.

For the GF channel, we analytically calculate the complete hard factor matrix for the process $H^{GF}_{gg\to Hgg}$, at the NLO, using the helicity amplitudes given in Ref. [25], as suggested in Ref. [26]. The needed color basis for this calculation is identical to that for describing di-jet production in hadron-hadron collision, as given in Ref. [19]. The soft factor $\mathbf{S}_{ab\to Hcd}$ is also a matrix in the color space, and γ^s is the associated anomalous dimension for the soft factor, which can also be obtained from the result for di-jet production [19] by switching the Mandelstam variables $\hat{t}$ and $\hat{u}$ to $(\hat{t}_1+\hat{t}_2)/2$ and $(\hat{u}_1+\hat{u}_2)/2$, respectively. The Sudakov form factor $\mathcal{S}_{\rm Sud}$ resums the leading double logarithms and the sub-leading logarithms, which is

$$S_{\rm Sud}(s,\hat{\mu},b_*) = \int_{b_0^2/b_*^2}^{\hat{\mu}^2} \frac{d\mu^2}{\mu^2}\left[\ln\left(\frac{s}{\mu^2}\right)A + B + D\ln\frac{s}{P_{J\perp 1}^2R^2} + D\ln\frac{s}{P_{J\perp 2}^2R^2}\right], \tag{7}$$

where the coefficients A, B and D can be expanded perturbatively in α_s, and they are defined as $A=\sum_i A^{(i)}\left(\frac{\alpha_s}{\pi}\right)^{(i)}$, $B=\sum_i B^{(i)}\left(\frac{\alpha_s}{\pi}\right)^{(i)}$ and $D=\sum_i D^{(i)}\left(\frac{\alpha_s}{\pi}\right)^{(i)}$. For GF process, $gg\to Hgg$ process at the NLO, we have $A=C_A\frac{\alpha_s}{\pi}$, $B=-2C_A\beta_0\frac{\alpha_s}{\pi}$ and $D=C_A\frac{\alpha_s}{2\pi}$. For VBF process, $qq\to Hqq$ process at the NLO, we have $A=C_F\frac{\alpha_s}{\pi}$, $B=-3/2C_F\frac{\alpha_s}{\pi}$ and $D=C_F\frac{\alpha_s}{2\pi}$. The coefficients A and B come from the energy evolution effect in the TMD PDFs [15], so that they only depend on the flavor of the incoming partons and are independent of the scattering process. The coefficient D is derived from the soft factor associated with the final state jet. It quantifies the effect of soft radiation which goes outside the jet cone, hence it depends on the jet size R. Since our calculation is based on the small cone size approximation, only the term proportional to $\log(1/R^2)$ is kept in the final expression of the Sudakov factor of Eq. (7), which describes the $q_\perp$ distribution. The b-space variable $b_*=b/\sqrt{1+b^2/b_{\rm max}^2}$ with $b_{\rm max}=1.5\ {\rm GeV}^{-1}$, which make the lower limit in the Sudakov integrand to be larger than the scale Λ_{QCD} and all the pieces in it can be calculated by the perturbative QCD theory. Consequently, a non-perturbative factor $e^{-\mathcal{F}_{NP}(Q^2,b)}$ has to be added to model the non-perturbative contribution arising from the large b-region. In this work, we choose the non-perturbative formalism presented in Ref. [27], which however only affects the prediction in extreme small $q_\perp$ region ($q_\perp<1$ GeV).

3. Numerical analysis

We apply the above resummation formula to compute the $q_\perp$ distributions of the Higgs boson production associated with two high energy jets. In our numeric calculations, we have included the $A^{(2)}$ contribution at the two-loop order [28] in the Sudakov form factor, in addition to the $A^{(1)}$, $B^{(1)}$ and $D^{(1)}$ contributions discussed above. This is because the coefficient $A^{(2)}$ only depends on the flavor of the incoming partons, and not on the scattering process. Besides, we have included a theta-function $\Theta(\hat{\mu}-q_\perp)$ in Eq. (3) to limit the range of $q_\perp$ integration, because the resummation formula is only valid in the region of $q_\perp<\hat{\mu}$. Based on the study in Ref. [20], we choose resummation scale $\hat{\mu}=P_{J\perp}^{lead}$ or $\hat{\mu}=P_{J\perp}^{sub}$ in this work to estimate the theoretical uncertainty, where $P_{J\perp}^{lead}$ and $P_{J\perp}^{sub}$ are the transverse momenta of the final state leading jet and sub-leading jet, respectively. The resummation scale can be chosen arbitrarily, however, we should use the typical scale in the processes in order to reduce the impact of missing higher-order contributions. This process is dominated by double t-type channel, and the typical scale is the jet $P_{J\perp}$. Therefore, we choose the jet $P_{J\perp}$ as the resummation scale in our prediction. The uncertainty from the choice of $\hat{\mu}$ will decrease after we include higher order corrections in the hard factor. In addition, we take the mass of the Higgs boson (m_H) to be 125 GeV, and set the renormalization scale related to the $\alpha_s(\tilde{\mu})$ in the hard factor to $\tilde{\mu}=m_H$ in this study, with the CT14 NNLO PDFs [29]. Following the experimental analysis [30], we require the rapidity of the observed jets to satisfy $|y_J|<4.4$. We use the anti-k_t algorithm to define the observed jets, and the jet size and the minimal transverse momentum are set at $R=0.4$ and $P_{J\perp}>30$ GeV, which are similarly used in the experimental analysis [30]. In our calculation we have applied the narrow jet approximation [31]. We have also constrained the two final state jets to have a large rapidity separation with $|\Delta y_{JJ}|>2.6$, which was applied in experimental analysis to enhance VBF contribution. Hence, we applied this cut in both VBF and GF channels for comparison. In order to enhance VBF contribution, the di-jet invariant mass cut is also applied in some LHC measurements, however it is already largely included by the cut on Δy_{JJ}, since a large Δy_{JJ} implies a large di-jet invariant mass. Hence, we do not consider it in this work.

Finally, we compare in Fig. 1 the predictions from our resummation calculation, the fixed order calculation, and the MC event generator Pythia8. A noticeable difference is found in the shape of the $q_\perp$ distribution, predicted from our resummation calculation, for the VBF and GF production processes. The peak position for the VBF process is around 5 GeV, while for the GF process, it is around 30 GeV. This is because the sub-leading logarithm in the VBF production process can become large, as analyzed in Ref. [21], which can then push the peak position of the $q_\perp$ distribution to a much smaller value than that in the GF production process. Hence, the GF contribution can be largely suppressed, as compared to the VBF contribution, by requiring $q_\perp$ to be small in the Higgs boson plus two jet events produced at the LHC. To further compare the Pythia8 predictions against ours, besides the $q_\perp$ differential cross sections in the first two plots of Fig. 1, we also show their normalized distributions in the third and fourth plots. It is evident that Pythia8 predicts a flatter shape than ours, and another significant disagreement lies in the peak position of the $q_\perp$ distribution from the VBF production process. Pythia8 predicts a peak in $q_\perp$ around 10 GeV, while ours is at about 5 GeV. We notice that the shape of $q_\perp$ distribution is not sensitive to the choice of $\hat{\mu}$ for the VBF contribution, which leads to a small theoretical uncertainty band in the normalized $q_\perp$ distribution, as shown in the third panel of Fig. 1. In contrast, the relatively large theoretical uncertainties in the normalized $q_\perp$ distribution for the GF contribution, as shown in the fourth panel of Fig. 1, arise from the stronger $\hat{\mu}$ dependence in predicting the shape of $q_\perp$ distribution. Comparing to pythia8 predictions, there is a small shoulder for the resummation result in the third plot of Fig. 1 around 30 GeV. It is because the Y piece peaks around the same region. In that region, both resummation and fixed-order contributions are important. The resummation calculation contains an all order contribution, while the Y piece only takes account of $Y^{(1)}$, so there is a mismatch between them. Such non-physical behavior could come from this mismatch, however

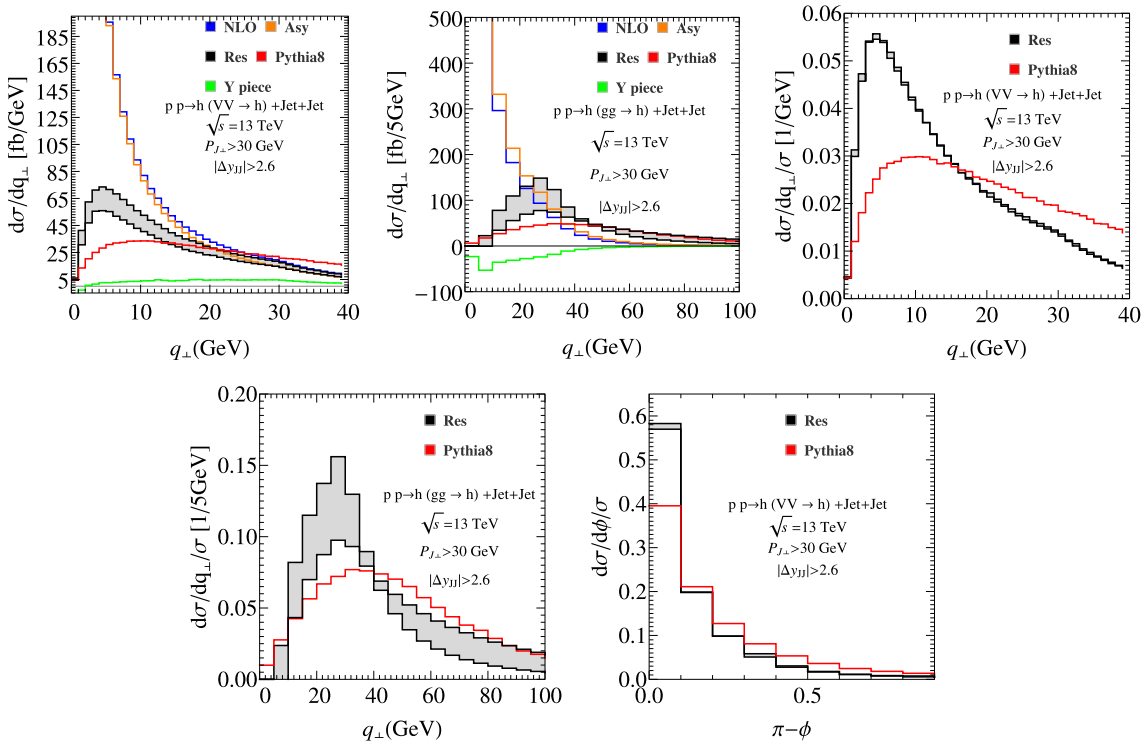

Fig. 1. The differential cross sections of Higgs boson plus two jet production at the LHC as functions of $q_\perp$ and azimuthal angle ϕ between Higgs boson and the final state two-jet system. In these plots, "NLO" is fixed order prediction at the next-to-leading order and it is the tree level of Higgs plus three partons production; "Asy" stands for the asymptomatic behavior of fixed order computations at low transverse momentum $q_\perp$; "Y"-piece represents the difference between the full results from the fixed order calculations and the asymptotic results; "Res" is the final resummation result; "Pythia8" is the predictions from Pythia8. In the GF channel, we only consider the dominant gluon-gluon scattering contribution in this work. The α_s order Y pieces are included in the resummation curves. The predictions from Pythia8 are based on the tree level scattering amplitudes with parton showers. The uncertainty of our resummation calculation is estimated by varying the resummation scale $\hat{\mu}$ from $P_{J\perp}^{lead}$ to $P_{J\perp}^{sub}$.

Table 1
The predicted kinematic acceptances for the azimuthal angle cut-off in the Higgs boson plus two jet production at the LHC.

Cut-off $(\pi - \phi)$	<0.2	<0.3	<0.4	<0.5	<0.54
Res VBF	78.15∼76.77%	88.00∼86.59%	93.09∼92.43%	95.85∼95.49%	96.53∼96.50%
Pythia8 VBF	60.64%	73.35%	81.45%	86.80%	88.44%

further studies are needed to resolve this issue. We will show all the details about these in a long version of this paper.

In the fifth plot of Fig. 1, we also show the distribution of the azimuthal angle ϕ between the Higgs boson and the final state jet pair which is calculated by integrating all the possible phase space except for constraining the ϕ value within a certain bin region. Such differential cross section is also sensitive to the soft gluon radiation and the Higgs boson production mechanism. Requiring a large separation in this azimuthal angle could largely suppress the GF contribution, but not the VBF contribution. The experimentalists at the LHC have already applied this technique to enhance the fraction of VBF contribution in their data, after imposing some proper kinematic cuts [30], in order to measure the coupling of Higgs boson to weak gauge bosons. To this aim, a precise theoretical evaluation of the kinematic acceptance after imposing the kinematic cuts is needed. In Ref. [30], the ATLAS Collaboration required the azimuthal angle separation (ϕ) between the Higgs boson and the di-jet system to be $\phi > 2.6$, and compared the measured fiducial cross section with the Pythia8 prediction. Below, we shall compare the predicted kinematic acceptance from Pythia8 to our resummation calculation. As shown in Table 1, the predicted kinematic acceptance with $\phi > 2.84$ is larger by about 14% in our resummation calculation than in Pythia8. For $\phi > 2.6$, they differ by about 8%, and our resummation calculation results in a larger total fiducial cross section. This implies a larger value in the coupling of Higgs boson to weak gauge bosons by about 4%. At the High-Luminosity LHC, with an integrated luminosity of up to 3000 fb^{-1}, the expected precision on the measurement of the production cross section of the SM-like Higgs boson via VBF mechanism is around 10% [32]. Hence, the difference found in our resummation and Pythia8 calculations of the fiducial cross sections could become important. Further comparisons on various event shapes between the experimental data and our resummation predictions could also be carried out in order to test the Standard Model and to search for New Physics.

4. Summary

In summary, we have applied the TMD resummation theorem to study the production of the Higgs boson associated with two inclusive jets at the LHC. Based on the TMD factorization formalism, all the factors are calculated up to the NLO. Our work provides a framework for applying the TMD resummation calculation to other $2 \to 3$ scattering processes. More importantly, this is the first time in the literature the effect from multiple soft gluon radiation is studied for this production channel of the Higgs boson at the NLL order, which brings the accuracy of theoretical prediction into a new stage. We find large difference between the Pythia8

and our predictions in the distributions of the total transverse momentum ($q_\perp$) and the azimuthal angle (ϕ) correlations of the final state Higgs boson and two-jet system, after imposing the kinematic cuts used in the LHC data analysis. Although in this work, we only consider the $gg \to Hgg$ channel for the GF process, as ref. [21] showed, the $q_\perp$ distribution shapes for all channels in the GF process are almost same, therefore our conclusions based on the distribution shapes work for the whole GF process. In this paper, we only compare the resummation result with Pythia8 predictions. A comparison with predictions from other parton shower methods is also desired. But this is beyond the scope of the present paper, and we leave that for future work.

At the end of this paper, we would like to discuss the non-global logarithms in the Higgs boson plus jet production processes. The non-global logarithms are found to be important in some processes. (See, e.g., a recent review in Ref. [33].) They appear at two-loop order, which is beyond the scope of the current paper. How to deal with the non-global logarithms in the Higgs boson plus jet production processes remains to be investigated. We hope to come back to this issue in the future.

Acknowledgements

We would like to thank Joshua Isaacson, Bin Yan and Kirtimaan Mohan for helpful discussion. This work is partially supported by the U.S. Department of Energy, Office of Science, Office of Nuclear Physics, under contract number DE-AC02-05CH11231, and by the U.S. National Science Foundation under Grant No. PHY-1719914. C.-P. Yuan is also grateful for the support from the Wu-Ki Tung endowed chair in particle physics.

References

[1] G. Aad, et al., ATLAS Collaboration, Phys. Lett. B 716 (2012) 1.
[2] S. Chatrchyan, et al., CMS Collaboration, Phys. Lett. B 716 (2012) 30.
[3] G. Aad, et al., ATLAS Collaboration, arXiv:1407.4222 [hep-ex].
[4] G. Aad, et al., ATLAS Collaboration, arXiv:1408.3226 [hep-ex].
[5] G. Aad, et al., ATLAS Collaboration, arXiv:1408.7084 [hep-ex].
[6] J.M. Campbell, R.K. Ellis, G. Zanderighi, J. High Energy Phys. 0610 (2006) 028, arXiv:hep-ph/0608194.
[7] J.M. Campbell, R.K. Ellis, R. Frederix, P. Nason, C. Oleari, C. Williams, J. High Energy Phys. 1207 (2012) 092, arXiv:1202.5475 [hep-ph].
[8] T. Figy, C. Oleari, D. Zeppenfeld, Phys. Rev. D 68 (2003) 073005, arXiv:hep-ph/0306109.
[9] See, for example, R.K. Ellis, W.T. Giele, G. Zanderighi, Phys. Rev. D 72 (2005) 054018, arXiv:hep-ph/0506196; Phys. Rev. D 74 (2006) 079902, Erratum.
[10] S. Dittmaier, S. Dittmaier, C. Mariotti, G. Passarino, R. Tanaka, S. Alekhin, J. Alwall, E.A. Bagnaschi, et al., arXiv:1201.3084 [hep-ph];
S. Heinemeyer, et al., LHC Higgs Cross Section Working Group Collaboration, arXiv:1307.1347 [hep-ph].
[11] K. Arnold, et al., Comput. Phys. Commun. 180 (2009) 1661, https://doi.org/10.1016/j.cpc.2009.03.006, arXiv:0811.4559 [hep-ph].
[12] J.R. Forshaw, M. Sjodahl, J. High Energy Phys. 0709 (2007) 119, https://doi.org/10.1088/1126-6708/2007/09/119, arXiv:0705.1504 [hep-ph].
[13] R. Kleiss, W.J. Stirling, Phys. Lett. B 200 (1988) 193, https://doi.org/10.1016/0370-2693(88)91135-5.
[14] J.C. Collins, D.E. Soper, G.F. Sterman, Nucl. Phys. B 250 (1985) 199.
[15] X. Ji, J.P. Ma, F. Yuan, Phys. Rev. D 71 (2005) 034005; J. High Energy Phys. 0507 (2005) 020.
[16] J. Collins, Foundations of Perturbative QCD, Cambridge Monographs on Particle Physics, Nuclear Physics and Cosmology, vol. 32, 2011.
[17] J.C. Collins, D.E. Soper, Nucl. Phys. B 193 (1981) 381; Erratum: Nucl. Phys. B 213 (1983) 545;
J.C. Collins, D.E. Soper, Nucl. Phys. B 197 (1982) 446.
[18] H.X. Zhu, C.S. Li, H.T. Li, D.Y. Shao, L.L. Yang, Phys. Rev. Lett. 110 (8) (2013) 082001;
H.T. Li, C.S. Li, D.Y. Shao, L.L. Yang, H.X. Zhu, Phys. Rev. D 88 (2013) 074004.
[19] P. Sun, C.-P. Yuan, F. Yuan, Phys. Rev. Lett. 113 (23) (2014) 232001; Phys. Rev. D 92 (9) (2015) 094007.
[20] P. Sun, J. Isaacson, C.-P. Yuan, F. Yuan, Phys. Lett. B 769 (2017) 57, https://doi.org/10.1016/j.physletb.2017.02.037.
[21] P. Sun, C.-P. Yuan, F. Yuan, Phys. Lett. B 762 (2016) 47.
[22] S. Dawson, Nucl. Phys. B 359 (1991) 283.
[23] G. Bozzi, S. Catani, D. de Florian, M. Grazzini, Nucl. Phys. B 737 (2006) 73.
[24] A. Mukherjee, W. Vogelsang, Phys. Rev. D 86 (2012) 094009.
[25] S. Badger, E.W. Nigel Glover, P. Mastrolia, C. Williams, J. High Energy Phys. 1001 (2010) 036.
[26] I. Moult, I.W. Stewart, F.J. Tackmann, W.J. Waalewijn, Phys. Rev. D 93 (9) (2016) 094003.
[27] P. Sun, J. Isaacson, C.-P. Yuan, F. Yuan, arXiv:1406.3073 [hep-ph].
[28] S. Catani, D. de Florian, M. Grazzini, Nucl. Phys. B 596 (2001) 299;
S. Catani, L. Cieri, D. de Florian, G. Ferrera, M. Grazzini, Nucl. Phys. B 881 (2014) 414.
[29] S. Dulat, et al., Phys. Rev. D 93 (3) (2016) 033006, https://doi.org/10.1103/PhysRevD.93.033006.
[30] ATLAS Collaboration, ATLAS-CONF-2016-067;
M. Aaboud, et al., ATLAS Collaboration, Phys. Rev. D 98 (2018) 052005.
[31] M. Furman, Nucl. Phys. B 197 (1982) 413;
F. Aversa, P. Chiappetta, M. Greco, J.P. Guillet, Nucl. Phys. B 327 (1989) 105; Z. Phys. C 46 (1990) 253;
D. de Florian, W. Vogelsang, Phys. Rev. D 76 (2007) 074031.
[32] CMS Collaboration, CMS-PAS-FTR-16-002.
[33] T. Becher, M. Neubert, L. Rothen, D.Y. Shao, J. High Energy Phys. (1611) 019; Erratum: J. High Energy Phys. 1705 (2016) 154, 2017.